Original paper

Biomechan Model Mechanobiol 2 (2003) 21 – 36 © Springer-Verlag 2003
DOI 10.1007/s10237-002-0025-9

Average hydroxyapatite concentration is uniform in the extracollagenous ultrastructure of mineralized tissues: evidence at the 1–10-μm scale

C. Hellmich, F.-J. Ulm

Abstract At the ultrastructural observation scale of fully mineralized tissues ($\ell = 1 - 10$ μm), transmission electron micrographs (TEM) reveal that hydroxyapatite (HA) is situated both within the fibrils and extrafibrillarly, and that the majority of HA lies outside the fibrils. The extrafibrillar amount of HA varies from tissue to tissue. By means of mathematical modeling, we here provide strong indications that there exists a physical quantity that is the same inside and outside the fibrils, for all different fully mineralized tissues. This quantity is the average mineral concentration in the non-collagenous space. This space is the sum of the extrafibrillar volume and of the volume of the fibrils that is not occupied by collagen molecules. Two independent sets of experimental observations covering a large range of tissue mass densities establish the relevance of our proposition: (i) mass density measurements and diffraction spacing measurements, re-analyzed through a dimensionally consistent packing model; (ii) optical density measurements of TEMs. The aforementioned average uniform HA-concentration in the extracollagenous space of the ultrastructure may emphasize the putative role played by a number of non-collagenous organic molecules in providing the chemical boundary conditions for mineralization of HA in the extracollagenous space. The probable existence of an average uniform extracollagenous HA concentration has far-reaching consequences for the mechanical behavior of mineralized tissues.

Introduction

The hierarchical organization of bone and its mechanical implications have attracted researchers for hundreds of years. In the line of pertinent contributions in the field (Katz et al. 1984; Weiner and Wagner 1998), we here distinguish five levels of hierarchical organization:

1. The macrostructure at an observation scale of several mm to cm, where cortical (or compact) bone and trabecular (or spongy) bone can be distinguished (Fig. 1a, b).
2. The microstructure at an observation scale of several 100 μm to several mm, where cylindrical units called osteons build up cortical bone, and where the single trabecular struts or plates can be distinguished (Fig. 1c, d).

Received: 18 February 2002 / Accepted: 23 October 2002

C. Hellmich (✉), F.-J. Ulm
Department of Civil and Environmental Engineering,
Massachusetts Institute of Technology,
Cambridge, MA 02139, USA
e-mail: christian.hellmich@tuwien.ac.at

Present address: C. Hellmich
Institute for Strength of Materials,
Vienna University of Technology (TU Wien), 1140 Vienna, Austria

The authors gratefully acknowledge the financial support of this study by the Max Kade Foundation, New York, N.Y., mediated through the Austrian Academy of Sciences (ÖAW), Vienna, Austria, enabling the sabbatical leave of the first author from the Vienna University of Technology (TU Wien), Austria. In addition, they thank Lorna Gibson, Massachusetts Institute of Technology, Cambridge, USA, and Peter Fratzl, University of Leoben, Leoben, Austria, for helpful comments on the manuscript. Special thanks are due to Sidney Lees, The Forsyth Institute, Boston, USA, whose decade-long scientific work is the foundation for this research, and whose numerous constructive suggestions were highly appreciated.

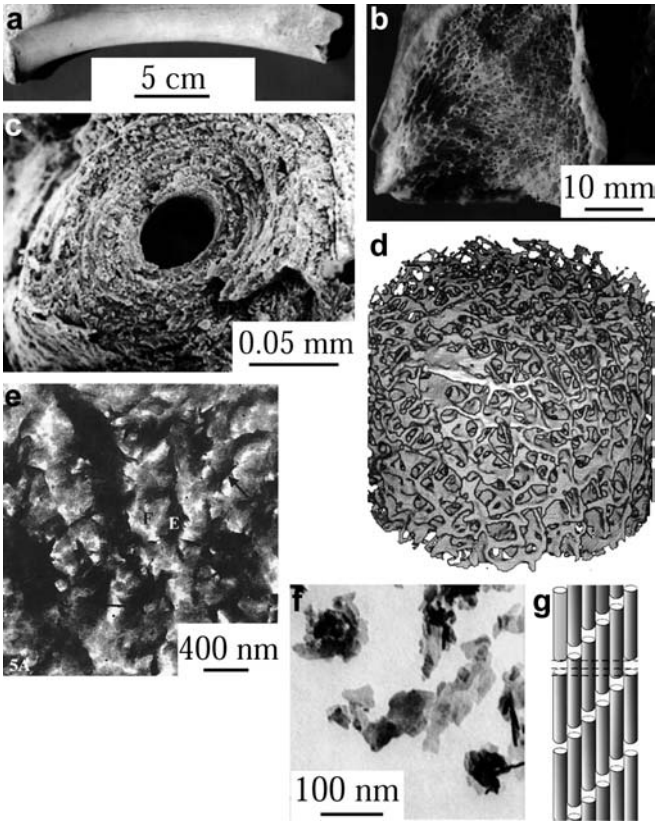

Fig. 1a–g. Hierarchical organization of bone: **a** whole long bone (macrostructure); **b** section through long bone (macrostructure); **c** osteon (microstructure); **d** trabecular spaceframe (microstructure); **e** ultrastructure; **f** HA crystals (elementary components); **g** collagen molecules (elementary components). *Sources*: **a–c, f, g** from Weiner and Wagner (1998), with permission of Annual Reviews, www.AnnualReviews.org; **d** from Luo et al. (1999), reprinted with permission of Elsevier Science, Copyright 1999 by World Federation of Ultrasound in Medicine and Biology; **e** from Prostak and Lees (1996), reprinted with permission of Springer-Verlag, p. 478, Fig. 5a

3. The ultrastructure (or extracellular solid bone matrix) at an observation scale of 1–10 μm, comprising the material building up both trabecular struts and osteons (Fig. 1e).
4. Within the ultrastructure, collagen-rich domains (light areas in Fig. 1e) and collagen-free domains (dark areas in Fig. 1e) can be distinguished at an observation scale of several hundred nanometers. Commonly, these domains are referred to as fibrils and extrafibrillar space.
5. Finally, at an observation scale of several tens of nanometers, the so-called elementary components of mineralized tissues can be distinguished. These are:

   – Plate or needle-shaped mineral crystals consisting of impure HA (Ca_{10} $[PO_4]_6$ $[OH]_2$) with typical 1–5 nm thickness, and 25–50 nm length (Weiner and Wagner 1998) (Fig. 1f);
   – Long cylindrically shaped collagen molecules with a diameter of about 1.2 nm and a length of about 300 nm (Lees 1987), which are self-assembled in staggered organizational schemes (fibrils) with characteristic diameters of 50–500 nm (Cusack and Miller 1979; Miller 1984; Lees et al. 1990, 1994b; Weiner et al. 1997; Weiner and Wagner 1998; Rho et al. 1998a; Prostak and Lees 1996), (Fig. 1g). Several covalently bonded fibrils are sometimes referred to as fibers;
   – Different non-collagenous organic molecules, predominantly lipids and proteins (Urist et al. 1983; Hunter et al. 1996);
   – Water.

The organization the elementary components within the ultrastructure of mineralized tissues (bone and mineralized tendons) has provoked some controversy. While the organization of collagen into fibrils and fibers according to the Hodge–Petruska scheme (Hodge and Petruska 1963) was more or less agreed on, the predominant location of the mineral crystals remained unclear for some time. Katz and Li (1973) estimated that at least 80% of the mineral is intrafibrillar. This motivated intensive research on how the mineral can be deposited in fibrils. This research was often based on TEMs (Traub et al. 1989; Landis et al. 1991, 1996; Weiner and Wagner 1998). However, the calculations in (Katz and Li 1973) were based on the assumption that the average lateral distance between collagen molecules would be the same for mineralized and unmineralized tissues. In the mid-1980s, Lees and coworkers (Lees et al. 1984; Bonar et al. 1985; Lees 1986) have shown by neutron diffraction studies that the average lateral distance of the collagen molecules does change upon demineralization. In fact, it increases. This is why Katz and Li (1973) have overestimated the intrafibrillar mineral content—it

must be smaller than 80%. The first model incorporating the dependence of the average collagen distance on the mineralization degree of the tissue was the pioneering generalized packing model of Lees (Lees et al. 1984; Lees 1986, 1987), an extension of the hexagonal lattice model of Hulmes and Miller (Hulmes and Miller 1979; Miller 1984). Lees' model clearly indicated that the majority of the minerals lie outside the fibrils. This was independently corroborated by TEMs (Lees et al. 1994b; Prostak and Lees 1996) and by micromechanical considerations (Pidaparti et al. 1996). More recently, Fratzl et al. (1996) and Hulmes et al. (1995) have developed computer models for the determination of the actual deviation of the collagen molecular organization from a perfect hexagonal lattice. Lees (1986) has already explained that—probably because of the crosslinks between collagen molecules acting predominantly between the ends of these molecules—at most 20% of the collagen molecules in a transverse section through a fibril are stereospecifically ordered. Still, hexagonal lattice-type models are relevant for the determination of average lateral distances between collagen molecules in a fibril.

Based on such average quantities we here investigate a hypothesis for the mineral concentration in both the fibrillar and the extrafibrillar space of the ultrastructure of bone and mineralized tendon:

– *The average HA concentration is uniform in the extracollageneous ultrastructure of mineralized tissues.*

Hypothesis

The present paper focusses on the ultrastructural level of all collagenous mineralized tissues, defined at an observation scale of 1–10 μm. In the special case of lamellar bone, the following developments refer to a single lamella with a characteristic thickness of 3–12 μm (Katz et al. 1984; Buckwalter et al. 1995; Weiner et al. 1997; Zylberberg et al. 1998). A more precise definition of our hypothesis (see the title of the paper) requires the definition of different spaces within the ultrastructural volume element V (Fig. 2):

– The space occupied by the collagen molecules, V_{coll}, Fig. 2b. Each collagen molecule is a triple helix structure which can be approximated by a cylinder with around 300 nm length, around 1.25 nm effective diameter (Miller 1984; Lees 1987) and a volume of $v_{\mathrm{coll}} = 335.6\ \mathrm{nm}^3$. Through self-assembly (Christiansen et al. 2000), the collagen molecules build up higher organizational units called fibrils, more or less cylindrical arrangements with diameters between 50 and 500 nm (Cusack and Miller 1979; Miller 1984; Lees et al. 1990, 1994b; Weiner et al. 1997; Weiner and Wagner 1998; Rho

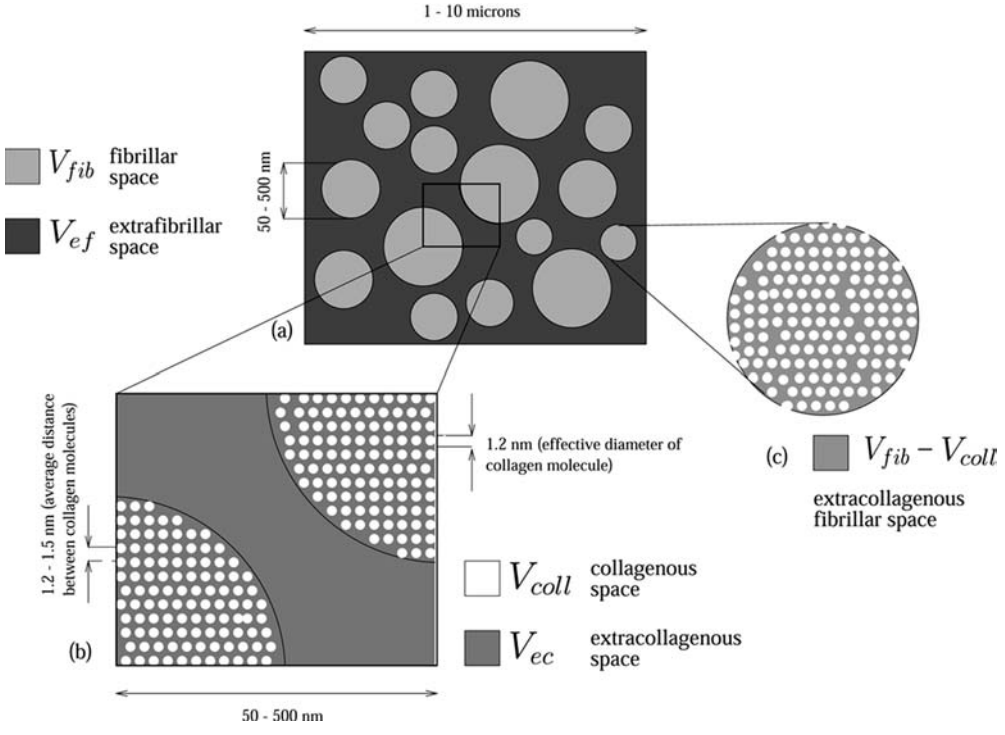

Fig. 2a–c. Schematical sketch of the spaces in the extracellular bone matrix or ultrastructure: **a** section through the ultrastructural representative volume element perpendicular to the direction of the fibrils; **b, c** close-ups (collagen molecules are not drawn to scale; since the collagen molecules are oriented perpendicular to the page, they appear as circles)

et al. 1998a; Prostak and Lees 1996), where the average lateral distance of two molecules (collagen spacing) is between 1.2 and 1.5 nm (Miller 1984; Bonar 1985; Lees et al. 1984). In the longitudinal direction, the collagen molecules obey a staggered scheme with axial macroperiod D (Hodge and Petruska 1963) (Fig. 4b); in the transverse direction, they are on the average hexagonally packed (Figs. 4a and 2).

- The fibrillar volume $V_{\mathrm{fib}} > V_{\mathrm{coll}}$, Fig. 2a, comprises all fibrils within the ultrastructural volume V. V_{coll} is a subspace of V_{fib}.
- The other subspace of V_{fib} is $(V_{\mathrm{fib}} - V_{\mathrm{coll}})$, Fig. 2c, the volume of the fibrils which is not occupied by collagen molecules. It may be called extracollagenous fibrillar volume, or non-collagenous fibrillar volume. Katz and Li (1973) call $(V_{\mathrm{fib}} - V_{\mathrm{coll}})$ "the space which is in collagen fibrils exclusive of the collagen molecules (intrafibrillar or intermolecular space)".
- The space within the ultrastructure which is not occupied by fibrils, is called extrafibrillar space, $V_{\mathrm{ef}} = V - V_{\mathrm{fib}}$, Fig. 2a. No collagen molecules are found in this space.
- The union of the spaces V_{ef} and $(V_{\mathrm{fib}} - V_{\mathrm{coll}})$, $V_{\mathrm{ec}} = V_{\mathrm{ef}} + (V_{\mathrm{fib}} - V_{\mathrm{coll}}) = V - V_{\mathrm{coll}}$, is the extracollagenous space, $V_{\mathrm{ec}} > V_{\mathrm{ef}}$, (Fig. 2b). Katz and Li (1973) call it "non-collagenous space". This term indicates that V_{ec} is the space in the ultrastructure that is not occupied by collagen molecules.

In principal, the tissue mineral can be present anywhere in V_{ec}, and it may be argued that it be rather concentrated in $(V_{\mathrm{fib}} - V_{\mathrm{coll}})$ on the one hand, or in V_{ef} on the other. We test here the hypothesis of an average uniform concentration of HA in V_{ec}, i.e., we test whether there is no difference between differently located average mineral concentrations,

$$\langle c_{\mathrm{HA}} \rangle_{V_{\mathrm{ef}}} \equiv \langle c_{\mathrm{HA}} \rangle_{(V_{\mathrm{fib}} - V_{\mathrm{coll}})} \quad . \tag{1}$$

In Eq. (1),

$$\langle (\cdot) \rangle_{V_i} = \frac{1}{V_i} \int\limits_{V_i} (\cdot)\, \mathrm{d}V_i$$

is the average of the quantity $(\cdot)$ in volume V_i, $i \in [V_{\mathrm{ef}}, (V_{\mathrm{fib}} - V_{\mathrm{coll}}), V_{\mathrm{ec}}]$, and c_{HA} denotes the HA concentration, the amount (i.e., number) of HA crystal units per volume which is at least one order of magnitude smaller than V_i.

From the standard relation between average quantities

$$\langle c \rangle_{V_{\mathrm{ec}}} = \langle c \rangle_{(V_{\mathrm{fib}} - V_{\mathrm{coll}})} \frac{V_{\mathrm{fib}} - V_{\mathrm{coll}}}{V_{\mathrm{ec}}} + \langle c \rangle_{V_{\mathrm{ef}}} \frac{V_{\mathrm{ef}}}{V_{\mathrm{ec}}} \tag{2}$$

it follows that Eq. (1) implies the equality

$$\langle c_{\mathrm{HA}} \rangle_{V_{\mathrm{ef}}} \equiv \langle c_{\mathrm{HA}} \rangle_{V_{\mathrm{ec}}} \quad . \tag{3}$$

Multiplication of Eq. (3) with the molar mass of HA, $\mathscr{M}_{\mathrm{HA}}$, renders our hypothesis in terms of apparent mass densities, $\rho^{\star,\mathrm{i}}_{\mathrm{HA}} = \mathscr{M}_{\mathrm{HA}} \langle c_{\mathrm{HA}} \rangle_{V_i}$, $i \in [\mathrm{ef}, \mathrm{ec}]$,

$$\rho^{\star,\mathrm{ef}}_{\mathrm{HA}} = \mathscr{M}_{\mathrm{HA}} \langle c_{\mathrm{HA}} \rangle_{V_{\mathrm{ef}}} = \frac{M^{\mathrm{ef}}_{\mathrm{HA}}}{V_{\mathrm{ef}}} \equiv \rho^{\star}_{\mathrm{HA}}, \mathrm{ec} = \mathscr{M}_{\mathrm{HA}} \langle c_{\mathrm{HA}} \rangle_{V_{\mathrm{ec}}} = \frac{M_{\mathrm{HA}}}{V_{\mathrm{ec}}} \quad , \tag{4}$$

where $M^{\mathrm{ef}}_{\mathrm{HA}}$ is the mineral mass in the extrafibrillar space, and M_{HA} is the total mineral mass in the ultrastructural volume element. Contrary to average concentrations $\langle c_{\mathrm{HA}} \rangle_{V_i}$, apparent mass densities $\rho^{\star,i}_{\mathrm{HA}}$ are directly accessible from chemical experiments (Lees et al. 1979, 1987; Lees and Page 1992; Blitz and Pellegrino 1969). Equation (4) expresses the following: "Within V, the extrafibrillar mineral mass divided by the extrafibrillar volume is equal to the total mass of HA divided by the part of V that is not occupied by collagen molecules".

Proof

In order to "prove" our hypothesis by experimental data, we express it in terms of the relative amount of mineral located extrafibrillarly, $\phi_{\mathrm{HA,ef}} = M^{\mathrm{ef}}_{\mathrm{HA}} / M_{\mathrm{HA}}$. This is mathematically achieved by multiplying Eq. (4) by $V_{\mathrm{ef}}/M_{\mathrm{HA}}$:

$$\phi_{\mathrm{HA,ef}} = \frac{M^{\mathrm{ef}}_{\mathrm{HA}}}{M_{\mathrm{HA}}} = \frac{\rho^{\star}_{\mathrm{HA,ef}}}{\rho^{\star}_{\mathrm{HA}}} \equiv \frac{V_{\mathrm{ef}}}{V - V_{\mathrm{coll}}} = \frac{vf_{\mathrm{ef}}}{1 - vf_{\mathrm{coll}}} \quad . \tag{5}$$

Here, $vf_{\mathrm{ef}} = V_{\mathrm{ef}}/V$ is the extrafibrillar volume fraction, and $vf_{\mathrm{coll}} = V_{\mathrm{coll}}/V$ is the collagen volume fraction. $\rho^{\star}_{\mathrm{HA}} = M_{\mathrm{HA}}/V$ is the apparent mineral density referred to the reference volume V, and

$$\rho^{\star}_{\mathrm{HA,ef}} = M^{\mathrm{ef}}_{\mathrm{HA}}/V = \rho^{\star,\mathrm{ef}}_{\mathrm{HA}} \times vf_{\mathrm{ef}}$$

is the apparent density of the extrafibrillar mineral. Since Eq. (5) was derived from Eqs. (1)–(4) we can state:

- *If and only if the relative extrafibrillar mineral content* $\phi_{\mathrm{HA,ef}} = M^{\mathrm{ef}}_{\mathrm{HA}}/M_{\mathrm{HA}}$ *is equal to a certain ratio of volume fractions, namely* $vf_{\mathrm{ef}}/(1\text{-}vf_{\mathrm{coll}})$*, then HA is uniformly concentrated in the extrafibrillar space of mineralized tissues.*

We check this necessary and sufficient condition for the existence of a uniform extracollagenous mineral concentration in the following way:

- We determine $vf_{\mathrm{ef}}/(1 - vf_{\mathrm{coll}})$ from weighting experiments and diffraction spacing measurements (experimental set I), covering the whole mass density range of mineralized tissues.
- We determine $\rho^{\star}_{\mathrm{HA,ef}}/\rho^{\star}_{\mathrm{HA}}$ from an independent set of measurements (experimental set II), namely optical density measurements of TEMs of three very different mineralized tissues with low, medium, and high mass density.
- We compare the values for $\rho^{\star}_{\mathrm{HA,ef}}/\rho^{\star}_{\mathrm{HA}}$ of these three tissues with values for $vf_{\mathrm{ef}}/(1 - vf_{\mathrm{coll}})$ of identical or similar tissues.
- The almost perfect agreement of the compared values, which are derived from two independent sets of experimental observations, will deliver the "proof" of our hypothesis. (It is not a proof in the strictest sense since, in principle, there could exist experimental values (which we do not know presently) not fulfilling (Eq. 5).)

Experimental set I: mass, volume, and distance measurements

We are interested in determining the extrafibrillar mineral content through the volume fractions (i.e., the right hand side of Eq. 5):

$$\phi_{\mathrm{HA,ef}} = \frac{vf_{\mathrm{ef}}}{1 - vf_{\mathrm{coll}}} \quad . \tag{6}$$

The collagen volume fraction $vf_{\mathrm{coll}} = V_{\mathrm{coll}}/V$ is simply the ratio of apparent-to-real collagen mass density:

$$vf_{\mathrm{coll}} = \frac{\rho^{\star}_{\mathrm{coll}}}{\rho_{\mathrm{coll}}} \quad , \tag{7}$$

with $\rho^{\star}_{\mathrm{coll}} = M_{\mathrm{coll}}/V$ and $\rho_{\mathrm{coll}} = M_{\mathrm{coll}}/V_{\mathrm{coll}}$; M_{coll} denotes the mass of collagen in V. The real mass density of (molecular) type I collagen, ρ_{coll}, can be determined from different independent tests. On the one hand, (almost) all components except collagen can be removed from bone, tendon, or skin tissue. Robinson (1960) and Bear (1956) determined the mass density of dehydrated, decalcified cortical bone, and Pomoroy and Mitton (1951) determined the mass density of dried calf skin. On the other hand, Chotia (1975) provided a model for the organization of proteins in general, based on structural invariants like the volumes occupied by different residues. Harley et al. (1977) applied this model to rat-tail tendon for different hydration states. The state of complete dehydration refers to molecular type I collagen. All these different authors report very similar values of $\rho_{\mathrm{coll}} = 1.41 - 1.45$ g/cm^3. This indicates the existence of a general value for ρ_{coll}, independent of the tissue type. Following the pioneering calculations of Katz and Li (1973), p. 9, and Lees (1987), p. 290, we here adopt a value of $\rho_{\mathrm{coll}} = 1.41$ g/cm^3. For the determination of $\rho^{\star}_{\mathrm{coll}}$, we use the fact that collagen constitutes approximately 90% by weight of the organic matter in mineralized tissues (Blitz and Pellegrino 1969; Urist et al. 1983; Lees 1987; Weiner and Wagner 1998):

$$M_{\mathrm{coll}} = 0.9 \times M_{\mathrm{org}}; \quad \rho^{\star}_{\mathrm{coll}} = 0.9 \times \rho^{\star}_{\mathrm{org}} \ , \tag{8}$$

where M_{org} is the mass of organic matter in V, and $\rho^{\star}_{org} = M_{org}/V$ is the apparent organic mass density. $\rho^{\star}_{org}$ can be determined from weighting experiments on demineralized and dehydrated specimens (Blitz and Pellegrino 1969; Lees et al. 1979; Lees 1987; Lees and Page 1992), harvested from different anatomical locations of different vertebrates at different ages, see also the Appendix. There, data from bone and mineralized tendon specimens of fish, amphibia, reptiles, birds, and mammals, covering the entire mass density of mineralized tissues, are compiled.

On the other hand, the determination of the extrafibrillar volume fraction $vf_{ef} = 1 - vf_{fib}$ in Eq. (6) requires quantification of the fibrillar space within the mineralized tissue. This can be achieved by application of a model for the organization of collagen. While there exists an impressive amount of models for the organization of unmineralized collagen (for a comprehensive review, see Fratzl et al. (1993) and Hulmes et al. (1995)), the literature on collagen organization in mineralized tissues is to our knowledge rather scarce. In this study, for the sole purpose of determining the fibrillar volume fraction $vf_{fib} = V_{fib}/V$, we will use Lees' (1984) generalized packing model (Lees et al. 1984; Bonar et al. 1985; Lees 1987), as the simplest model to quantify the average crosslink length between collagen molecules. In average, collagen molecules obey to certain packing patterns (Hulmes and Miller 1979), which stem from crosslinks between the macromolecules, which are situated presumably at the ends of these molecules (Eyre et al. 1984; Bailey et al. 1998), Fig. 4b. (Between the ends of the macromolecules, however, the single molecules are free to undergo all different kinds of deformation. The resulting large degree of lateral disorder can be reasonably simulated by a fluid-like lateral arrangement of collagen molecules (Fratzl et al. 1993).) The packing of collagen in different mineralized tissues can be characterized by the equatorial diffraction spacing d_w, obtained from neutron diffraction experiments (Lees et al. 1984; Bonar et al. 1985), Fig. 4a. Most remarkably, Lees (1987) provides evidence that there exists a unique relation between d_w and the wet bone density ρ_w, for specimens harvested from different anatomical locations of different animals at different ages (Fig. 3). Actually, ρ_w was measured at the microstructural level–cortical bone specimens with 2 mm characteristic length (Lees et al. 1985; Bonar et al. 1985)–but this value equals approximately the ultrastructural mass density value. Cortical bone has a microporosity φ of less than 5% (Sietsema 1995). The relation between the mass density of wet cortical bone, $\rho_{w,m}$, and that of wet solid bone matrix (ultrastructure), $\rho_{w,u}$, is given by $\rho_{w,m} = \rho_{w,u}(1-\phi) + \rho_{H_2O}\phi$ with $\rho_{H_2O} = 1\,\mathrm{g/cm^3}$ as the mass density

a

tissue	ρ_w[g/cm^3]	d_w[nm]
cow bone matrix	1.13	1.53
fish clythrum	1.43	1.38
turkey tendon	1.59	1.33
turkey tendon	1.66	1.34
deer antler	1.78	1.29
cow tibia	2.04	1.24

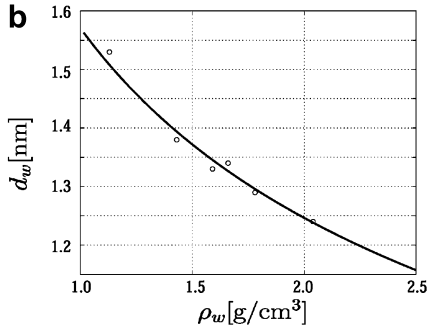

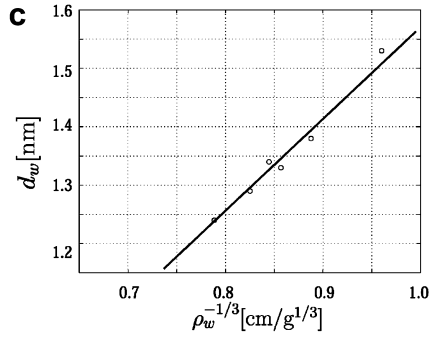

Fig. 3a–c. Equatorial diffraction spacing d_w as a function of wet tissue density ρ_w: **a** experimental data compiled by Lees (1987); **b** $d_w - \rho_w$ – plot, **c** $d_w - \rho_w^{-1/3}$-plot illustrates the existence of a dimensionless constant; $d_w \propto \rho_w^{-1/3}$ ($r^2 = 98\%$)

of water. For $\varphi = 0.05$, we have $\rho_{w,m}/\rho_{w,u} = 0.98$; i.e., $\rho_{w,u}$ and $\rho_{w,m}$ vary from each other by at most 2%, which is the precision of the calculations we report here.

What is most surprising about Lees' experimental finding illustrated in Fig. 3 is that the two quantities involved are defined on different levels: the equatorial diffraction spacing d_w is a local distance of 1.2–1.5 nm between collagen molecules in a fibril; while ρ_w is a quantity defined at the level of 1–10 μm. Following dimensional analysis (Buckingham 1914; Barenblatt 1996), it appears that if a physically meaningful relation exists between only these two parameters, it must be of the form (Carneiro 2000):

$$\frac{d_w}{m_0^{1/3}\rho_w^{-1/3}} = \text{const} \quad . \tag{9}$$

For const $\times\, m_0^{1/3} = 1.57 \times 10^{-10}\,\text{kg}^{1/3}$, we get the excellent fit of Fig. 3b, c ($r^2 = 0.98$), with m_0 of dimension mass. d_w enters the generalized packing model of Lees (1984) for the average equatorial organization of collagen (Fig. 4a).

Figure 4b shows the meridional organization: in a staggered scheme with unit length (or axial macroperiod) $D \approx 64$ nm, $4.4 \times D$ long macromolecules are separated by $0.6 \times D$ hole zones (Hodge and Petruska 1963). From Fig. 4, the volume of one rhomboidal fibrillar organizational unit is seen to be:

$$v_{fib} = b d_w 5D \quad , \tag{10}$$

with $b = 1.47$ nm as one average (rigid) crosslink length, see Fig. 4a. If we denote by v_{coll} the volume of one collagen macromolecule, the volume fraction of fibrils, $vf_{fib} = V_{fib}/V$, is obtained from the collagen volume fraction multiplied by the volume ratio v_{fib}/v_{coll}:

$$vf_{fib} = vf_{coll} \times \frac{v_{fib}}{v_{coll}}; \quad v_{coll} = \frac{\mathscr{M}_{coll}/N_A}{\rho_{coll}} = 335.6\,\text{nm}^3 \quad , \tag{11}$$

where $\mathscr{M}_{coll} = 285\,\text{kg/mol}$ is the molar mass of collagen (Lees 1987; Miller 1984), and $N_A = 6.022 \times 10^{23}\ \text{mol}^{-1}$ is Avogadro's number. Accounting for Eqs. (7)–(11), the extrafibrillar volume fraction, $vf_{ef} = 1 - vf_{fib}$, reads as

$$vf_{ef} = 1 - 0.9\rho^*_{org} \times \frac{\text{const} \times m_0^{1/3}\rho_w^{-1/3} b \times 5D \times N_A}{\mathscr{M}_{coll}} \quad . \tag{12}$$

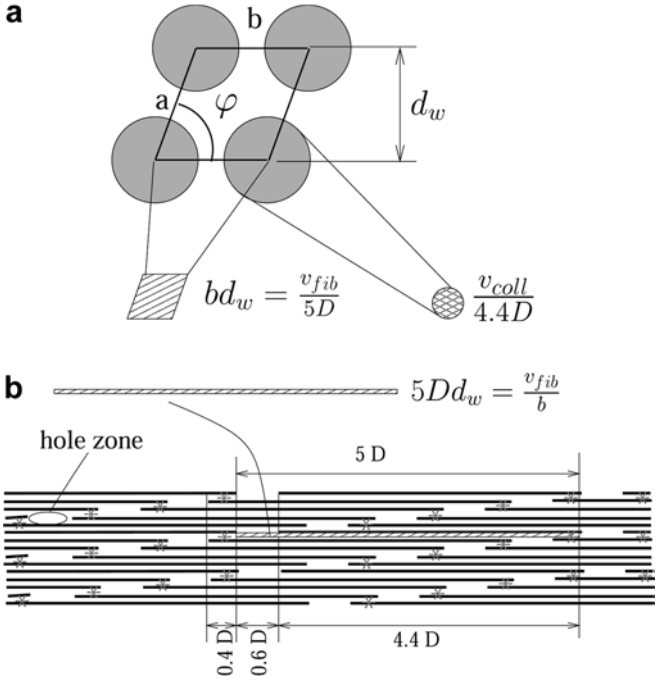

Fig. 4a, b. Organization of type I collagen molecules in mineralized tissues. **a** Average equatorial organization according to Lees (Lees et al. 1984; Lees 1986, 1987); two constant average crosslink lengths, $a = 1.52$ nm and $b = 1.47$ nm, are the sides of a rhomboidal unit cell with non-constant angle φ and volume v_{fib}; the diffraction spacing is $d_w = a \times \sin\varphi$; **b** Meridional organization according to the Hodge–Petruska scheme (Hodge and Petruska 1963; Bailey et al. 1998); D is the axial macroperiod; *asterisk* represents crosslink sites; one cylindrical collagen molecule has volume v_{coll} and length 4.4 D

In Eq. (12), $\rho^{\star}_{org}$ and ρ_w are tissue-specific values, given in the Appendix, whereas const $\times$ m_0, b, D, N_A, and $\mathscr{M}_{coll}$ are constants, which were previously defined. Figure 5 illustrates Eq. (12) in the form of ($vf_{ef}|\rho_w$)-data pairs. Insertion of expression (12) together with Eqs. (7) and (8) into Eq. (6) provides a first assessment of the relative amount of extrafibrillar mineral, from mass density and distance measurements.

$$\phi_{HA,ef} = \frac{1 - vf_{coll}(\rho^{\star}_{org}) \times \frac{v_{fib}[d_w(\rho_w)]}{v_{coll}}}{1 - vf_{coll}\left(\rho^{\star}_{org}\right)} = \frac{1 - 0.9\rho^{\star}_{org} \times \frac{\text{const} \times m_0^{1/3} \rho_w^{-1/3} b \times 5D \times N_A}{\mathscr{M}_{coll}}}{1 - 0.9\rho^{\star}_{org}/\rho_{coll}} \tag{13}$$

Note that the actual size of the individual fibrils (or possibly also fibers or fibril arrays of up to 1 μm diameter (Weiner and Wagner 1998)), as well as the number of fibrils within V, do not enter our analysis. Hence, it is not essential whether we refer to microfibrils, fibrils, or fibers in V_{fib}, provided that the average distance of collagen molecules within these higher organizational units is d_w. Figure 6 displays values of $\phi_{HA,ef}$ versus ρ_w for the experimental data set given in the Appendix. The high values of $\phi_{HA,ef}$ for the considered tissues indicate that the major part of mineral lies outside the fibrils. Still, in order to "prove" our assumption of a uniform mineral concentration in the extracollagenous space by means of Eq. (5), these values need to be confirmed by a second independent set of experimental observations. At the same time, this second set will also allow us to illustrate the relevance of the packing model developed here.

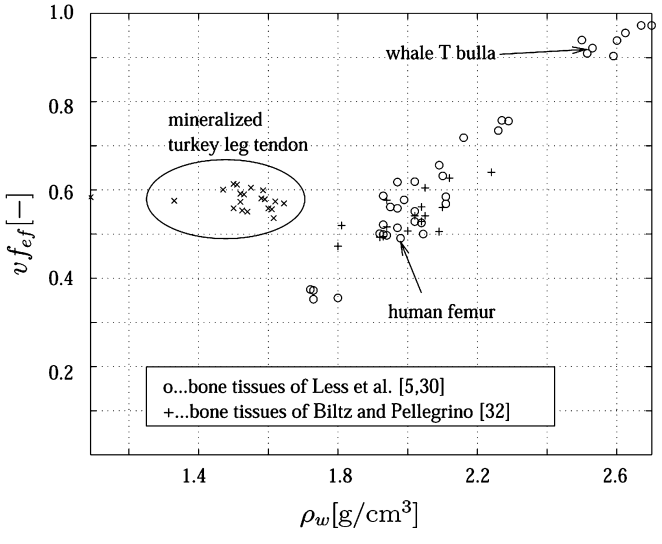

Fig. 5. Extrafibrillar volume fraction vf_{ef} as a function of wet tissue density ρ_w, calculated for experimental data given in the Appendix, by means of Eq. (12)

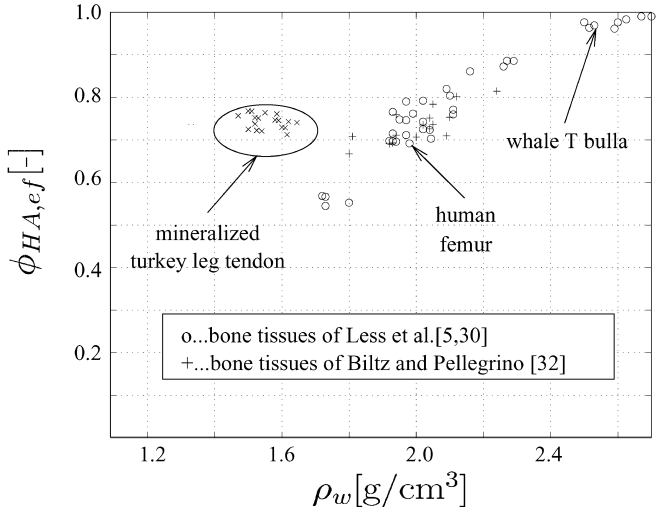

Fig. 6. Relative amount of extrafibrillar mineral (HA), $\phi_{HA,ef}$, as a function of wet tissue density ρ_w, calculated for experimental data given in the Appendix, by means of Eq. (13)

Experimental set II: optical density measurements of transmission electron micrographs

For the second set of observations we consider optical density measurements of TEMs.

Figure 7 displays three TEMs of cross sections of mineralized tissues, covering a wide range of wet bone mass densities; from $\rho_w = 1.5$ g/cm^3 for mineralized turkey leg tendon to $\rho_w = 2.6$ g/cm^3 for the rostrum of a whale. It is remarkable that the cylindrical morphology of the fibrils, extensively described in the open literature (see, for instance, Weiner and Wagner (1998)), seems rather characteristic for low mass density tissues like mineralized turkey leg tendon (Fig. 7a). As the mass density increases, the cylindrical organization structure becomes loose, e.g., in human bone (Fig. 7b), and degenerates to fibrillar sheets in high mass density bones like whale bone (Fig. 7c). TEMs show the electron density of material phases. The higher the electron density, the darker the respective area of the TEMs. Since HA exhibits by far the largest electron density of all elementary components, the TEMs displayed in Fig. 7 highlight that HA is mainly located outside the fibrils. We want to quantify the relative amount of extrafibrillar mineral, $\phi_{HA,ef}$, now defined by the left-hand side of Eq. (5):

$$\phi_{HA,ef} = \frac{\overset{*}{\rho}_{HA,ef}}{\overset{*}{\rho}_{HA}} = \frac{M^{ef}_{HA}}{M_{HA}}. \tag{14}$$

To this end, we will assume that the TEM cross sections displayed in Fig. 7 are representative for the entire tissue, i.e., that the displayed features are independent of the longitudinal direction. In other words, the fibrils are considered to be aligned perpendicular to the plane of the image. In the case of lamellar bone where different collagen orientations occur, a representative image must show parts of only one lamella, a with characteristic thickness of 3–12 μm (Katz et al. 1984; Buckwalter 1995; Weiner et al. 1997; Zylberberg et al. 1998; Zysset et al. 1998). By definition (Weiner et al. 1997, p. 509), one lamella "is made up of arrays of collagen fibrils which are more or less parallel to each other". The TEM-image of Fig. 7b, referring to lamellar bone, obviously shows parts of one lamella.

Let ω be the relative optical density, which is equal to 0 for a white pixel and to 1 for a black one. For the determination of ω, we adapt the protocol of Lees et al. (1994b): the TEM-images are scanned from a hardcopy of the references (Prostak and Lees 1996; Zylberberg et al. 1998), and then captured

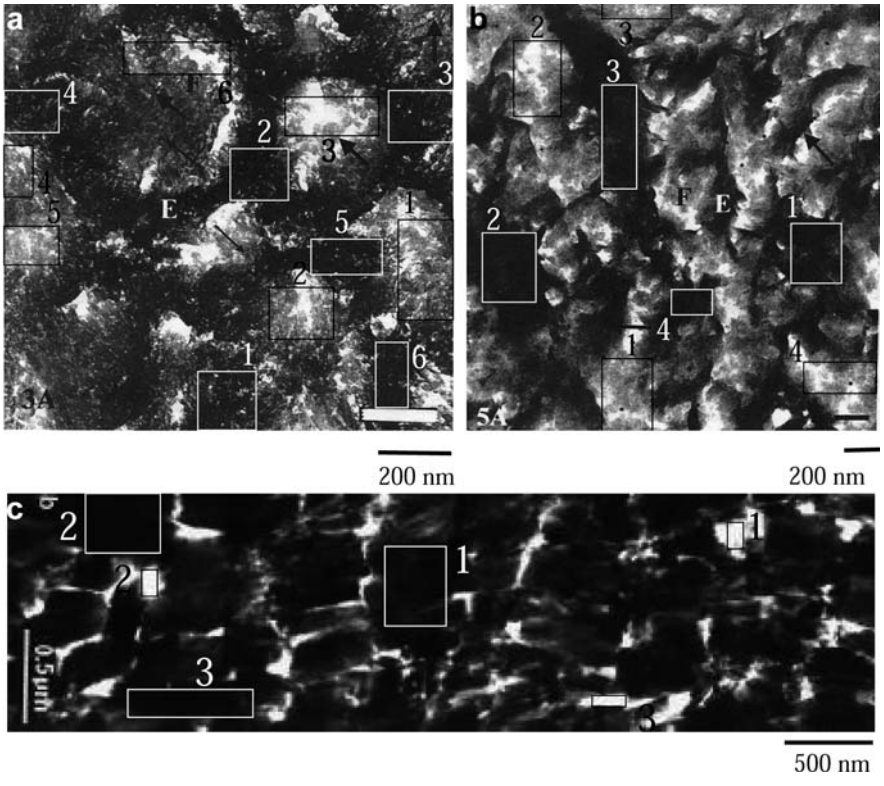

Fig. 7a–c. Transmission electron micrographs of cross sections through: **a** mineralized turkey leg tendon (Prostak and Lees 1996); **b** human tibia (Prostak and Lees 1996), (permission for reproduction granted by Springer-Verlag), and **c** whale rostrum (Zylberberg et al. 1998), (permission for reproduction forthcoming from Elsevier Science); F shows fibrils; E is extrafibrillar space; numbers indicate integration domains

by a frame grabber (Bradley 1994) and converted to a two-dimensional matrix with typical size of, e.g., 651×665 elements for Fig. 7a. The conversion is performed by MATLAB (Hunt et al. 2001). The elements of the matrix are total numbers $\mathscr{G}$, between 0 and 255, according to the unsigned byte array format for grey level pictures. These numbers are related to the relative optical density ω by

$$\omega(\mathbf{x}) = \frac{255 - \mathscr{G}(\mathbf{x})}{255} \quad , \tag{15}$$

where the two-dimensional vector $\mathbf{x}$ locates the position of a pixel in a TEM picture. Following Lees et al. (1994b, p. 184), it is assumed that the optical density is linearly proportional to the number of electrons transmitted through the particular area, and that the number of electrons is linearly proportional to the local HA mass density, $\hat{\rho}_{\mathrm{HA}}$, which is defined at an observation scale of some nanometers. Mathematically speaking,

$$\hat{\rho}_{\mathrm{HA}}(\mathbf{x}) = C_\rho \omega(\mathbf{x}) \quad . \tag{16}$$

C_ρ is a "calibration constant" and depends on the voltage at which the microscope is operated. Eq. (16) implies the reasonable assumption that, for the applied voltage of 80–100 kV, HA is the only optically dense phase in the TEM images, i.e., organic components and water cannot be discerned in the images. Linear relationships between optical density and mineral content are also commonly used for the analysis of backscattered electron imaging (Roschger et al. 1998). Based on the local mass density $\hat{\rho}_{\mathrm{HA}}$ average mineral density values for both the fibrillar and the extrafibrillar space can be obtained from:

$$\langle \hat{\rho}_{\mathrm{HA}} \rangle_{\mathrm{fib}} = C_\rho \langle \omega \rangle_{\mathrm{fib}} \simeq \sum_{i=1}^{N} \frac{1}{\Omega_{\mathrm{fib},i}} \int\limits_{\Omega_{\mathrm{fib,i}}} C_\rho \omega(\mathbf{x}) \, \mathrm{d}\Omega \quad , \tag{17}$$

$$\langle \hat{\rho}_{\mathrm{HA}} \rangle_{\mathrm{ef}} = C_\rho \langle \omega \rangle_{\mathrm{ef}} \simeq \sum_{i=1}^{N} \frac{1}{\Omega_{\mathrm{ef},i}} \int\limits_{\Omega_{\mathrm{ef},i}} C_\rho \omega(\mathbf{x}) \, \mathrm{d}\Omega \tag{18}$$

$$\langle y \rangle_j = \frac{1}{\Omega_j} \int\limits_{\Omega_j} y \, \mathrm{d}\Omega$$

stands for the average of quantity y over domain Ω_j. Direct determination of $\langle \hat{\rho}_{\mathrm{HA}} \rangle_{\mathrm{fib}}$ and $\langle \hat{\rho}_{\mathrm{HA}} \rangle_{\mathrm{ef}}$ from the TEM images is very difficult because the boundaries between fibrillar and extrafibrillar regions are almost impossible to define. Therefore, we employ an approximation technique indicated in Eqs. (17) and (18). By means of the xv-framegrabber (Bradley 1994) we cut carefully chosen $2N$ rectangular areas out of each TEM image. N of these areas are regarded as either typically fibrillar (with areas $\Omega_{\mathrm{fib},i}$), or as typically extrafibrillar (with areas $\Omega_{\mathrm{ef},i}$): $N = 6$ for Fig. 7a, $N = 4$ for Fig. 7b, and $N = 3$ for Fig. 7c. Justification of our choice will be given in the form of a convergence study. Similar to (17) and (18), the average overall HA mass density can be obtained from:

$$\langle \hat{\rho}_{\mathrm{HA}} \rangle = \frac{1}{\Omega} \int\limits_{\Omega} C_\rho \omega(\mathbf{x}) \mathrm{d}\Omega = \mathbf{C}_\rho \langle \omega \rangle \quad , \tag{19}$$

with Ω denoting the entire picture domain. The average densities defined by Eqs. (17) and (18) are related to the apparent mineral densities $\rho^{*}_{\mathrm{HA,ef}}$ and ρ^{*}_{HA} by:

$$\rho^{*}_{\mathrm{HA,ef}} = vf_{\mathrm{ef}} \times \langle \hat{\rho}_{\mathrm{min}} \rangle_{\mathrm{ef}}; \rho^{*}_{\mathrm{HA}} = \langle \hat{\rho}_{\mathrm{HA}} \rangle = vf_{\mathrm{ef}} \langle \hat{\rho}_{\mathrm{HA}} \rangle_{\mathrm{ef}} + (1 - vf_{\mathrm{ef}}) \times \langle \hat{\rho}_{\mathrm{HA}} \rangle_{\mathrm{fib}} \quad . \tag{20}$$

Transformation of Eq. (20) allows for the determination of the extrafibrillar volume fraction vf_{ef} of tissues shown in TEM images:

$$vf_{\mathrm{ef}} = \frac{\langle \hat{\rho}_{\mathrm{HA}} \rangle - \langle \hat{\rho}_{\mathrm{HA}} \rangle_{\mathrm{fib}}}{\langle \hat{\rho}_{\mathrm{min}} \rangle_{\mathrm{ef}} - \langle \hat{\rho}_{\mathrm{HA}} \rangle_{\mathrm{fib}}} = \frac{\langle \omega \rangle - \langle \omega \rangle_{\mathrm{fib}}}{\langle \omega \rangle_{\mathrm{ef}} - \langle \omega \rangle_{\mathrm{fib}}} \quad . \tag{21}$$

vf_{ef} turns out to be 60% for the mineralized turkey leg tendon micrograph of Fig. 7a ($\rho_{\mathrm{w}} = 1.5$ g/cm^3), 53% for the human tibia ($\rho_{\mathrm{w}} = 2$ g/cm^3, Fig. 7b), and 85% for the whale rostrum ($\rho_{\mathrm{w}} = 2.6$ g/cm^3, Fig. 7c). From Fig. 5 it can be seen that these values are in perfect agreement with the values from the packing model, when we compare very similar tissues. The agreement is still good, when we compare the whale rostrum image to the whale T bulla packing model results.

Use of Eqs. (20) and (21) in Eq. (14) provides the sought quantitative assessment of the relative extrafibrillar mineral content, only from optical density measurements of TEMs:

$$\phi_{\mathrm{HA,ef}} = \left(1 - \frac{\left(\langle\omega\rangle - \langle\omega\rangle_{\mathrm{ef}}\right) \times \langle\omega\rangle_{\mathrm{fib}}}{\left(\langle\omega\rangle - \langle\omega\rangle_{\mathrm{fib}}\right) \times \langle\omega\rangle_{\mathrm{ef}}}\right)^{-1} . \tag{22}$$

Notably, the expression for $\phi_{\mathrm{HA,ef}}$ does not depend on C_ρ, i.e., on the calibration of the electron microscope. This enables us to compare in a consistent fashion the TEM-images shown in Fig. 7, obtained from different sources and different conditions.

For the three tissues displayed in Fig. 7, Fig. 8 illustrates the fast convergence of $\phi_{\mathrm{HA,ef}}$ for increasing numbers of domains cut out of the respective TEM. This fast convergence indicates a uniform thickness of the TEMs, and, in this respect, the high quality of the images. Furthermore, the fast convergence shows that a relative small number of chosen areas, $N \epsilon [3, 6]$, is sufficient to determine $\phi_{\mathrm{HA,ef}}$ with a precision of $[\phi_{\mathrm{HA,ef}}(N) - \phi_{\mathrm{HA,ef}}(N-1)] / \phi_{\mathrm{HA,ef}}(N) \epsilon [0.1\%;1.6\%]$, and that these areas were representative for the fibrillar as well as for the extrafibrillar space. The comparison of $\phi^{\mathrm{ef}}_{\mathrm{HA}} = 74\%$ for Fig. 7a (turkey leg tendon), which we scanned from the hardcopy of the paper by Prostack and Lees (1996) before we converted it by means of the frame grabber (Bradley 1994), with the value of 70–75%, which Lees et al. (1994b) determined directly from the TEM negatives of turkey leg tendon tissue, may give further confidence in our TEM evaluation protocol.

Finally, Table 1 summarizes the values of $\phi_{\mathrm{HA,ef}}$ assessed respectively from the weighting experiments, through Eq. (13), and from TEM optical density measurements, through Eq. (22). The values almost coincide, and the slight difference may be attributed to the fact that the two series of experimental samples are very similar, but still not identical. This good accordance of values obtained from two independent assessment methods (Eq. (5) indeed holds) provides the sought after evidence that the average HA concentration is uniform in the extracollagenous space of mineralized tissues: The average extracollagenous HA concentration is the same inside and outside the fibrils.

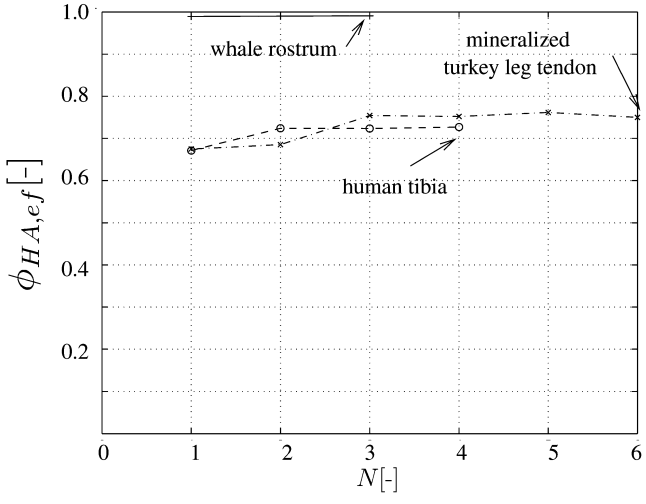

Fig. 8. Relative extrafibrillar mineral content of three different tissues, determined on the basis of N rectangular domains cut out of the TEM pictures of Fig. 7

Table 1. Percentage of HA outside fibrils: Results from mass density and distance measurements, and from optical density measurements of transmission electron micrographs

Tissue	ρ_{w} (g/cm^3)	$\phi_{\mathrm{HA,ef}}$ from packing model	$\phi_{\mathrm{HA,ef}}$ from TEM
Min. turkey leg tendon	1.5	74%	75%
Human femur (24 year old)	1.98	69%	
Human tibia (69 year old)	≈2		73%
Whale T bulla	2.53	97%	
Whale rostrum	2.60		99%

Discussion

This work concerns the distribution of HA in the ultrastructure of fully mineralized tissues, such as mineralized tendons and bone. In the case of lamellar bone, our approach is limited to the material building up one lamella. Mechanical structure–function relationships are well beyond the scope of this work. Furthermore, we evaluate merely average concentrations and apparent mass densities of HA in different subspaces of the ultrastructure, but not the distribution and organization of the bone mineral within these subspaces.

We have found a strong indication that the average HA concentration is uniform in the extracollagenous ultrastructure of mineralized tissues. This remarkable result appears to challenge the widely accepted view (Glimcher 1984) that collagen plays a significant role in the HA biomineralization process. However, from our results, we can only conclude that, in the asymptotic mineralization state, the possible specific influence of collagen can no longer be recorded in different tissues, such as human tibia, turkey leg tendon, and whale rostrum.

Early stages of mineralization have primarily been studied by means of TEMs. Numerous references (Traub et al. 1989, p.9824, Fig. 4; Landis et al. 1991, p.192), show images of longitudinal sections through various fibrils, or a longitudinal view on one fibril (Landis et al. 1991, pp. 188 and 190). These images indicate that preliminary mineralization starts within the hole regions (see Fig. 4b) between the ends of two collagen molecules. In these TEM images, showing longitudinal sections through the tissues, extrafibrillar and fibrillar spaces hide each other and are difficult to discern. This motivates a closer inspection of the TEM images of transverse sections of mineralizing tissues, as e.g., the ones produced by Landis et al. (1996) for turkey leg tendon. The upper image of Fig. 5 on p. 28 of the aforementioned reference shows five nucleation spots in the extrafibrillar space (all indicated with arrows), and two spots within a fibril (not indicated). Landis et al. (1996) emphasize the vicinity of these spots to fibrillar surfaces. From another perspective, the aforementioned distribution of "multiple, spatially and temporally independent" (Landis et al. 1996) nucleation spots (five extrafibrillar ones versus two intrafibrillar ones, $\phi_{\mathrm{HA,ef}} \approx 5/7 = 71\%$) accords well (at least approximately) with our suggestion of an average uniform mineral concentration, resulting in 74% extrafibrillar mineral, even during an early stage of mineralization. The very thought of average uniform mineral concentration even during early stages of mineralization would not be expected if the biochemists only found the collagen molecules to be active in the support or inhibition of the mineralization process of HA. Interestingly enough, in the course of time, the effect of non-collagenous proteins, proteoglycans, and lipids in tissue biomineralization has been increasingly emphasized (Urist 1983; Arsenault 1991; Hunter et al. 1996). These molecules may be absorbed to crystal surfaces, bound to collagen, or situated freely in the liquid environment between HA and collagen.

Consequently, the experimental evidence reported in the open literature does not contradict the suggestion that the HA biomineralization is controlled mainly by non-collagenous proteins, and that the role of collagen is a rather minor one. This would imply that the mineralization of HA would occur regardless of its location in the extracollagenous space, leading to an average uniform extracollagenous mineral concentration, strong indications for the existence of which we have presented in this paper.

In view of these considerations, we suggest that each of each of the elementary components (collagen, water, non-collagenous organic matter, HA) fulfills distinctive tasks:

- Collagen molecules condition the morphology of the ultrastructure, i.e., the organization around higher organizational units than single molecules. The morphology, which varies from cylindrical fibrils to fibrillar sheets, appears to be determined by the amount of collagen, and the latter may well be determined by the intensity and frequency of osteoblastic (or fibroblastic) activity. The formation of the collagen fibrils, however, is an exclusively chemical phenomenon (called "self-assembly"), driven by forces between the ends of the molecules, resulting in tight electrostatic or covalent cross links (Christiansen et al. 2000).
- Water provides the liquid environment for the biochemical activity of the non-collagenous organic matter.
- The non-collagenous organic matter, regulates HA mineralization, probably by proteins supporting or inhibiting mineralization, possibly also by lipids (Urist 1983; Arsenault 1991; Hunter et al. 1996). In this respect, there are far more questions than answers on the exact role of the involved cells (osteoclasts, osteoblasts, osteocytes, and lining cells in bone, fibroblasts in tendon, and chondrocytes in calcified cartilage).
- Finally, besides the metabolic function of HA as calcium storage, minerals in the extracollagenous space contribute to the mineralized tissues' mechanical stiffness and strength. The high disorder of

HA crystallites in mineralized tissues (Fratzl 1996), as well as the uniformity of their distribution throughout the extracollagenous space shown here, suggest an isotropic contribution of the HA crystals to the ultrastructural stiffness. Evidence for this suggestion is gained from the evaluation (Hellmich and Ulm 2002a) of two independent types of mechanical and chemical experiments (Lees et al. 1983, 1990, 1994a, 1995; Lees 1987): (1) A continuous dependence of the radial normal stiffness on only the HA volume fraction, for both isotropic and anisotropic tissues, reflects the isotropic contribution of HA to the ultrastructural stiffness; (2) evaluation of ultrasonic measurements at MHz and GHz frequencies reveal that collagen does not contribute to the radial stiffness, but exclusively to the axial stiffness, inducing the tissues' anisotropy. This contribution probably stems from mechanical activation of collagen molecules by tight links (Glimcher 1984) to the isotropic HA crystal foam or mineral matrix (Benezra Rosen et al. 2002). In this context, the probable existence of the uniform extracollagenous HA concentration plays a central role. The number of activated collagen molecules (which unilaterally reinforce the crystal foam) depends linearly on this concentration, i.e., on $\rho_{\mathrm{HA}}^{*,\mathrm{ec}}$ (Hellmich and Ulm 2002a). This intrinsic material function, in turn, allows for prediction of the ultrastructural bone stiffness in the framework of continuum micromechanics (Hellmich and Ulm 2002b).

Appendix

This appendix contains data from weighting experiments of dehydrated and demineralized tissue specimens from cortical bone and mineralized tendon. Part of the apparent densities used in this paper can be calculated from the tissue densities ρ_{w} and the weight fractions $WF_i = M_i/(M_{\mathrm{org}} + M_{\mathrm{H_2O}} + M_{\mathrm{HA}})$ provided by Lees (Lees et al. 1979, 1992; Lees 1987); through

$$\rho_i^* = M_i/V = WF_i \times \rho_{\mathrm{w}} \quad i \in \{\mathrm{min},\ \mathrm{org},\ \mathrm{H_2O}\} \ . \tag{A1}$$

$M_{\mathrm{H_2O}}$ is the mass of water in V. The first of following tables contains respective values used in this publication; values indicated as "mammalian tissue" are not further specified in the respective reference, and "MTLT" stands for "mineralized turkey leg tendon".

Second, the database of Biltz and Pellegrino (1969) was used. These authors give values for ρ_{w}, $vf_{\mathrm{H_2O}} = V_{\mathrm{H_2O}}/V$, and $WF_{\mathrm{Ca}}^{\mathrm{dry}}$, the weight fraction of calcium solved during the demineralization process, per unit mass of dry bone. From these quantities, $\rho_{\mathrm{H_2O}}^*$, ρ_{HA}^*, and ρ_{org}^* can be determined.

The apparent density of water, $\rho_{\mathrm{H_2O}}^*$, follows to be

$$\rho_{\mathrm{H_2O}}^* = \frac{M_{\mathrm{H_2O}}}{V} = \frac{M_{\mathrm{H_2O}}}{V_{\mathrm{H_2O}}} \times \frac{V_{\mathrm{H_2O}}}{V} = \rho_{\mathrm{H_2O}} \times vf_{\mathrm{H_2O}} \ , \tag{A2}$$

with the real density of water, $\rho_{\mathrm{H_2O}} = M_{\mathrm{H_2O}}/V_{\mathrm{H_2O}} = 1\mathrm{g/cm^3}$. Then, $WF_{\mathrm{Ca}}^{\mathrm{dry}}$ allows for the determination of the apparent density of calcium, $\rho_{\mathrm{Ca}}^* = M_{\mathrm{Ca}}/V$, M_{Ca} is the mass of calcium in V,

$$\rho_{\mathrm{Ca}}^* = WF_{\mathrm{Ca}}^{\mathrm{dry}} \times \left(\rho_{\mathrm{w}} - \rho_{\mathrm{H_2O}}^*\right) \ . \tag{A3}$$

For pure HA, $Ca_{10}(PO_4)_6(OH)_2$, ρ_{HA}^* is uniquely related to the apparent mass density of mineral by stoichiometry; $\rho_{\mathrm{HA}}^* = 2.59 \times \rho_{\mathrm{Ca}}^*$. However, biologically deposited HA is impure, i.e., a small, but significant amount of Ca-ions are substituted by lighter ions like Mg, Na, and K (Blitz and Pellegrino 1969; Rho et al. 1998b). Therefore, $\rho_{\mathrm{HA}}^*/\rho_{\mathrm{Ca}}^* > 2.59$. We estimate this ratio by comparison of two very similar samples from the databases of Lees (Lees et al. 1979; Lees and Page 1992; Lees 1987) and Biltz and Pellegrino (1969), respectively, i.e., the two rabbit bone samples, $\rho_{\mathrm{HA}}*/\rho_{\mathrm{Ca}}^* = 2.89$. Insertion of this ratio into Eq. (A3) allows for determination of ρ_{HA}^*, reading

$$\rho_{\mathrm{HA}}^* = 2.89 \times WF_{\mathrm{Ca}}^{\mathrm{dry}} \times (\rho_{\mathrm{w}} - \rho_{\mathrm{H_2O}}^*) \ . \tag{A4}$$

Insertion of Eq. (A4) into $\rho_{\mathrm{org}}^* = \rho_{\mathrm{w}} - \rho_{\mathrm{HA}}^* - \rho_{\mathrm{H_2O}}^*$ allows for determination of ρ_{org}^* ,

$$\rho_{\mathrm{org}}^* = (\rho_{\mathrm{w}} - \rho_{\mathrm{H_2O}}^*) \times (1 - 2.59 \times WF_{\mathrm{Ca}}^{\mathrm{dry}}) \ . \tag{A5}$$

The second of following tables contains respective values used in this publication.

Tissue	ρ_w (g/cm^3)	ρ^*_{HA} (g/cm^3)	ρ^*_{org} (g/cm^3)	$\rho^*_{H_2O}$ (g/cm^3)
MTLT[a]	1.47	0.63	0.32	0.51
MTLT[a]	1.50	0.65	0.32	0.54
MTLT[a]	1.50	0.60	0.36	0.54
MTLT[a]	1.51	0.65	0.32	0.54
MTLT[a]	1.52	0.65	0.33	0.53
MTLT[a]	1.52	0.67	0.35	0.50
MTLT[a]	1.52	0.58	0.37	0.58
MTLT[a]	1.53	0.66	0.34	0.54
MTLT[a]	1.54	0.69	0.37	0.48
MTLT[a]	1.55	0.73	0.33	0.50
MTLT[a]	1.58	0.73	0.35	0.51
MTLT[a]	1.58	0.74	0.33	0.51
MTLT[a]	1.59	0.73	0.35	0.51
MTLT[a]	1.60	0.75	0.37	0.48
MTLT[a]	1.61	0.72	0.37	0.52
MTLT[a]	1.61	0.78	0.39	0.45
MTLT[a]	1.62	0.78	0.36	0.49
MTLT[a]	1.65	0.81	0.36	0.48
Mammalian[b]	1.72	0.86	0.53	0.33
Deer antler[b]	1.73	0.88	0.54	0.31
Mammalian[b]	1.73	0.90	0.55	0.28
Mammalian[b]	1.80	0.94	0.56	0.31
Mammalian[b]	1.92	1.23	0.44	0.25
Mammalian[b]	1.93	1.22	0.44	0.27
Turkey tibia[b]	1.93	1.26	0.42	0.24
Mammalian[b]	1.93	1.24	0.37	0.33
Mammalian[b]	1.94	1.24	0.45	0.25
Mammalian[b]	1.95	1.33	0.39	0.23
Mammalian[b]	1.97	1.34	0.39	0.24
Mammalian[b]	1.97	1.28	0.34	0.35
Mammalian[b]	1.97	1.27	0.43	0.27
Human femur[b]	1.98	1.39	0.46	0.14
Mammalian[b]	1.99	1.37	0.38	0.24
Mammalian[b]	2.02	1.43	0.34	0.24
Mammalian[b]	2.02	1.41	0.40	0.20
Mammalian[b]	2.02	1.35	0.42	0.24
Cow tibia[c]	2.04	1.33	0.45	0.26
Mammalian[b]	2.04	1.39	0.43	0.22
Rat femur[b]	2.09	1.59	0.31	0.19
Rabbit femur[b]	2.10	1.53	0.34	0.23
Mammalian[b]	2.11	1.50	0.38	0.23
Mammalian[b]	2.11	1.51	0.38	0.22
Mammalian[b]	2.11	1.52	0.39	0.20
Bovine dentin[b]	2.16	1.66	0.26	0.24
Mammalian[b]	2.26	1.88	0.25	0.14
Horse petrosal[b]	2.27	1.84	0.23	0.20
Mammalian[b]	2.29	1.92	0.23	0.14
Mammalian[b]	2.50	2.35	0.06	0.09
Mammalian[b]	2.52	2.29	0.09	0.14
Whale T. Bulla[b]	2.53	2.33	0.08	0.13
Mammalian[b]	2.59	2.38	0.09	0.11
Mammalian[b]	2.60	2.44	0.06	0.10
Mammalian[b]	2.62	2.49	0.04	0.09
Mammalian[b]	2.67	2.59	0.03	0.05
Porpoise petrosal[b]	2.70	2.62	0.03	0.05

[a] Data from Lees and Page (1992)
[b] Data from Lees (1987)
[c] Data from Lees et al. (1979)

Tissue	ρ_w (g/cm^3)	ρ^*_{HA} (g/cm^3)	ρ^*_{org} (g/cm^3)	$\rho^*_{H_2O}$ (g/cm^3)
Fish	1.80	0.95	0.46	0.40
Turtle	1.81	1.02	0.42	0.37
Frog	1.93	1.13	0.45	0.35
Polar bear	1.92	1.14	0.45	0.33
Man	1.94	1.26	0.43	0.26
Elephant	2.00	1.36	0.44	0.20
Monkey	2.09	1.41	0.45	0.23
Cat	2.05	1.40	0.41	0.24
Horse	2.02	1.36	0.41	0.25
Chicken	2.04	1.37	0.43	0.24
Dog	1.94	1.28	0.38	0.28
Goose	2.04	1.41	0.40	0.23
Cow	2.05	1.43	0.36	0.26
Guinea pig	2.10	1.45	0.40	0.25
Rabbit	2.12	1.53	0.34	0.24
Rat	2.24	1.70	0.34	0.20

All data are taken from Biltz and Pellegrino (1969)

References

Arsenault, A.L.: Image analysis of collagen-associated mineral distribution in crytogenically prepared turkey leg tendons. Calcified Tissue Int 48 (1991) 56–62

Bailey, A.J.; Paul, R.G.; Knott, L.: Mechanisms of maturation and ageing of collagen. Mech Ageing Dev 106 (1998) 1–56

Barenblatt, G.I.: Scaling, self-similarity, and intermediate asymptotics. Cambridge University Press, Cambridge (1996)

Bear, R.S.: The structure of collagen molecules and fibrils. J Biophys Biochem Cytol 2 (1956) 363–368

Benezra Rosen, V.; Hobbs, L.W.; Spector, M.: The ultrastructure of anorganic bovine bone and selected synthetic hydroxyapatites used as bone graft substitute material. Biomaterials 23 (2002) 921–928

Biltz, R.M.; Pellegrino, E.D.: The chemical anatomy of bone. J Bone Joint Surg 51A (1969) 456–466

Bonar, L.C.; Lees, S.; Mook, H.A.: Neutron diffraction studies of collagen in fully mineralized bone. J Mol Biol 181 (1985) 265–270

Bradley, J.: Interactive image display for the x window system version 3.10a, 2nd edn. Available at http://www.trilon.com/xv/manual/xv-3.10a (1994)

Buckingham, E,: On physically similar systems. illustrations of the use of dimensional analysis. Phys Rev 4 (1914) 345–376

Buckwalter, J.A.; Glimcher, M.J.; Cooper, R.R.; Recker, R.: Bone biology. I: Structure, blood supply, cells, matrix, and mineralization. J Bone Joint Surg 77A (1995) 1256–1275

Carneiro, F.L.L.B.: On the use, by Einstein, of the principles of dimensional homogeneity in three problems of the physics of solids. Ann Braz Acad Sci 72 (2000) 591–596

Chothia, C: Structural invariants in protein folding. Nature 254 (1975) 304–308

Christiansen, D.L.; Huang, E.K.; Silver, F.H.: Assembly of type I collagen: fusion of fibril subunits and the influence of fibril diameter on mechanical properties. Matrix Biol 19 (2000) 409–420

Cusack, S.; Miller, A.: Determination of the elastic constants of collagen by Brillouin light scattering. J Mol Biol 135 (1979) 39–51

Eyre, D.R.; Paz, M.A.; Gallop, P.M.: Cross-linking in collagen and elastin. Ann Rev Biochem 53 (1984) 717–748

Fratzl, P.; Fratzl-Zelman, N.; Klaushofer, K.: Collagen packing and mineralization an X-ray scattering investigation of turkey leg tendon. Biophys J 64 (1993) 260–266

Fratzl, P.; Schreiber, S.; Klaushofer, K.: Bone mineralization as studied by small-angle X-ray scattering. Connect Tissue Res 34 (1996) 247–254

Glimcher, M.J.: Recent studies of the mineral phase in bone and its possible linkage to the organic matrix by protein bound phosphate bonds. Phil Trans R Soc Lond B Biol Sci, 304 (1984) 479–508

Harley, R.; James, D.; Miller, A.; White, JW.: Phonons and the elastic moduli of collagen and muscle. Nature 267 (1977) 285–287

Hellmich, Ch.; Ulm. F.-J.: Are mineralized tissues open crystal foams reinforced by crosslinked collagen? Some energy arguments. J Biomech 35 (2002a) 1199–1212

Hellmich, Ch.; Ulm. F.-J.: A micromechanical model for the ultrastructural stiffness of mineralized tissues. J Eng Mech 128 (2002b) 898–908

Hodge, A.J.; Petruska, J.A.: Recent studies with the electron microscope on ordered aggregates of the tropocollagen molecule. In: Ramachandran GN (ed.) Aspects of protein structure – Proceedings of a Symposium held in Madras 14–18 January 1963 and organized by the University of Madras, India. Academic Press, London, (1963) pp 289–300

Hulmes, D.J.S.; Miller, A.: Quasi-hexagonal molecular packing in collagen fibrils. Nature 282 (1979) 878–880

Hulmes, D.J.S.; Wess, T.J.; Prockop, D.J.; Fratzl, P.: Radial packing, order, and disorder in collagen fibrils. Biophys J 68 (1995) 1661–1670

Hunt, B.R.; Eipsman, R.L.; Rosenberg, J.M.: A guide to MATLAB for beginners and experienced users. Cambridge University Press, Cambridge (2001)
Hunter, G.K.; Hauschka, P.V.; Poole, A.R.; Rosenberg, L.C.; Goldberg, H.A.: Nucleation and inhibition of hydroxyapatite formation by mineralized tissue proteins. Biochem J 317 (1996) 59–64
Katz, E.P.; Li, S.-T.: Structure and function of bone collagen fibrils. J Mol Biol 80 (1973) 1–15
Katz, J.L.; Yoon, H.S.; Lipson, S.; Maharidge, R.; Meunier, A.; Christel, P.: The effects of remodelling on the elastic properties of bone. Calcif Tissue Int 36 (1984) S31–S36
Landis, W.J.; Hodgens, K.J.; Song, M.J.; Arena, J.; Kiyonaga, S.; Marko, M.; Owen, C.; McEwen, B.F.: Mineralization of collagen may occur on fibril surfaces: evidence from conventional and high-voltage electron microscopy and three-dimensional imaging. J Struct Biol 117 (1996) 24–35
Landis, W.J.; Moradian-Oldak, J.; Weiner, S.: Topographic imaging of mineral and collagen in the calcifying turkey tendon. Connect Tissue Res 25 (1991) 181–196
Lees, S.: Water content in type I collagen tissues calculated from the generalized packing model. Int J Biol Macromol 8 (1986) 66–72
Lees, S.: Considerations regarding the structure of the mammalian mineralized osteoid from viewpoint of the generalized packing model. Connect Tissue Res 16 (1987) 281–303
Lees, S.; Ahern, J.M.; Leonard, M.: Parameters influencing the sonic velocity in compact calcified tissues of various species. J Acoust Soc Am 74 (1983) 28–33
Lees, S.; Bonar, L.C.; Mook. H.A.: A study of dense mineralized tissue by neutron diffraction. Int J Biol Macromol 6 (1984) 321–326
Lees, S.; Hanson, D.; Page, E.A.: Some acoustical properties of the otic bones of a fin whale. J Acoust Soc Am 99 (1995) 2421–2427
Lees, S.; Hanson, D.; Page, E.A.; Mook, H.A.: Comparison of dosage-dependent effects of beta-aminopropionitrile, sodium fluoride, and hydrocortisone on selected physical properties of cortical bone. J Bone Miner Res 9 (1994a) 1377–1389
Lees, S.; Heeley, J.D.; Cleary, P.F.: A study of some properties of a sample of bovine cortical bone using ultrasound. Calcif Tissue Int 29 (1979) 107–117
Lees, S.; Page, E.A.: A study of some properties of mineralized turkey leg tendon. Connect Tissue Res 28 (1992) 263–287
Lees, S.; Pineri, M.; Escoubes, M.: A generalized packing model for type I collagen. Int J Biol Macromol 6 (1985) 133–136
Lees, S.; Prostak, K.S.; Ingle,V.K.; Kjoller, K.: The loci of mineral in turkey leg tendon as seen by atomic force microscope and electron microscopy. Calc Tissue Int 55 (1994b) 180–189
Lees, S.; Tao, N.-J.; Lindsay, M.: Studies of compact hard tissues and collagen by means of Brillouin light scattering. Connect Tissue Res 24 (1990) 187–205
Luo, G.; Kaufman, J.J.; Chiabrera, A.; Bianco, B.; Kinney, J.H.; Haupt, D.; Ryaby, J.T.; Siffert, R.S.: Computational methods for ultrasonic bone assessment. Ultrasound Med Biol 25 (1999) 823–830
Miller, A.: Collagen: the organic matrix of bone. Phil Trans R Soc Lond B Biol Sci 304 (1984) 455–477
Pidaparti, R.M.V.; Chandran, A.; Takano, Y.; Turner, C.H.: Bone mineral lies mainly outside the collagen fibrils: Predictions of a composite model for osteonal bone. J Biomech 29 (1996) 909–916
Pomoroy, C.D.; Mitton, R.J.: The real densities of chrome and vegetable tanned leather. J Soc Leather Trades Chem 35 (1951) 360–375
Prostak, K.S.; Lees, S.: Visualization of crystal-matrix structure. In situ demineralization of mineralized turkey leg tendon and bone. Calcif Tissue Int 59 (1996) 474–479
Rho, J.-Y.; Roy, M.E.; Tsui, T.Y.; Pharr, G.M.: Elastic properties of microstructural components of human bone tissue as measured by nanoindentation. J Biomed Mater Res 45 (1998a) 48–54
Rho, J.-Y.; Kuhn-Spearing, L.; Zioupos, P.: Mechanical properties and the hierarchical structure of bone. Med Eng Phys 20 (1998b) 92–102
Robinson, R.A.: Chemical analysis and electron microscopy of bone. In: Rodale K, Nicholson J, Brown E.M (eds) Bone as tissue. McGraw-Hill, New York, (1960) pp 186–250
Roschger, P.; Fratzl, P.; Eschberger, J.; Klaushofer, K.: Validation of quantitative backscattered electron imaging for the measurement of mineral density distribution in human bone biopsies. Bone 23 (1998) 319–326
Sietsema, W.K.: Animal models of cortical porosity. Bone 17 (1995) 297S–305S
Traub, W.; Arad, T.; Weiner, S.: Three-dimensional ordered distribution of crystals in turkey tendon collagen fibrils. Proc Natl Acad Sci USA, 86 (1989) 9822–9826
Urist, M.R.; DeLange, R.J.; Finerman, G.A.M.: Bone cell differentiation and growth factors. Science 220 (1983) 680–686
Weiner, S.; Arad, T.; Sabanay, I.; Traub, W.: Rotated plywood structure of primary lamellar bone in the rat: orientation of the collagen fibril arrays. Bone 20 (1997) 509–514
Weiner, S.; Wagner, H.D.: The material bone: structure – mechanical function relations. Ann Rev Mater Sci 28 (1998) 271–298
Zylberberg, L.; Traub, W.; de Buffrenil, V.; Allizard, F.; Arad, T.; Weiner, S.: Rostrum of a toothed whale: ultrastructural study of a very dense bone. Bone 23 (1998) 241–247
Zysset, P.K.; Goulet, R.W.; Hollister, S.J.: A global relationship between trabecular bone morphology and homogenized elastic properties. J Biomech Eng 120 (1998) 640–646